A numerical investigation of blast-structure interaction effects on primary blast injury risk and the suitability of existing injury prediction methods

J.W. Denny[a], G.S. Langdon[b], S.E. Rigby[b], A.S. Dickinson[a], J. Batchelor[c], L. Surey[c]

[a] Department of Mechanical Engineering, Faculty of Engineering and Physical Sciences, University of Southampton, UK

[b] Department of Civil and Structural Engineering, University of Sheffield, UK

[c] Clinical Informatics Research Unit, Faculty of Medicine, University of Southampton, UK

Abstract

Explosions increasingly occur in densely populated, urban locations. Primary blast injuries (PBIs), caused by exposure to blast wave overpressure, can be predicted using injury criteria, although many are based on idealised loading inputs. At present, no studies have analysed in detail how, and to what extent blast-structure interaction influences injury risk, and the suitability of injury criteria that assume ideal loading inputs. Computational fluid dynamics (CFD) was used to investigate shielding and channelling blast interaction effects involving a rigid corner and a wall, in comparison to the free-field scenario. Models examined the effects of structural-blast interaction on loading parameters at certain locations, the effect this has on expected PBIs, and the suitability and limitations of using available injury criteria. Blast wave interaction with the corner resulted in shielding that reduced peak overpressures by 43%-60% at locations behind the corner in comparison to the free-field scenario. Blast wave interaction with the corner and wall structure resulted in higher pressures and impulse due to channelling that significantly increased injury risk at the exposed location and reduced shielding behind the corner, in comparison to the corner alone. Blast interaction with the structures resulted in complex waveforms featuring multiple peaks and less clearly defined durations. In these cases, the application and interpretation of existing injury criteria had several limitations and reduced reliability. This numerical study demonstrates that structural-blast interaction has significant effect on PBI risk. Specific challenges and further work to develop understanding and reliability of injury prediction for urban blast scenarios are discussed.

Key words

Blast-structure interaction, building corner, injury criteria, numerical analysis, CFD, injury prediction, blast effects

1. Introduction

Explosions are increasingly occurring in densely populated locations due to the shifting nature of conflict into urban areas, terrorist attacks and industrial accidents such as the 2020 Beirut blast [1]. These can result in devastating injuries, with so-called “primary” blast injuries (PBIs) caused by exposure to the blast wave overpressure. Data from Action on Armed Violence has shown that when explosive weapons are used in towns and cities, 91% of casualties are civilians [2].

Urban environments comprise a large variety of geometries and layouts that can significantly alter the explosion effects and resulting blast injuries. Blast wave interaction in urban environments leads to reflection, shielding and channelling and in closed spaces, blast waves can reflect, ricochet, and coalesce [3]. Analysis of the 2004 Madrid Train Bombings demonstrated that confinement of explosions resulted in more serious injury outcomes [4]. At larger scales, analysis of the 2020 Beirut explosion demonstrated shielding and channelling effects caused by high-rise buildings [5].

Blast propagation and interaction phenomena arising in urban landscapes can be studied using modelling tools such as computational fluid dynamics (CFD). Models can be developed for specified blast scenarios, permitting examination of a wide range of blast effects at different scales, from individual buildings to broader cityscapes, at varying fidelities and sophistication. Modelled blast loading parameters can then be used to estimate blast injury risk or the expected spatial extent of casualties by referring to injury criteria.

Multiple criteria for primary blast injury (PBI) have been proposed to predict injury outcomes on a probabilistic basis depending on the blast conditions a person is exposed to. The most widely reported criteria are applicable to idealised blast waves, or ‘Friedlander’ [6] type waveforms that develop in open-field explosion scenarios. Alternative injury models have also been developed with applicability to non-ideal and complex blast waveforms, such as the Axelsson BTD model [7], which accounts for injuries to the respiratory tract, the thorax and the abdominal area, and the Weathervane SP model [8], reviewed in greater detail by Teland [9]. These models allow the input of non-ideal blast waves and predict injury in terms of an ‘Adjusted Severity of Injury Index’. These models have increased complexity and their accuracy is unknown in comparison to the injury criteria based on idealised blast wave inputs, with Teland suggesting that Axelsson-based methods are underpinned by poor quality data [9]. As a result, PBI criteria based on idealised (open-field) blast waveforms remain widely adopted.

It is widely understood that urban environments can modify blast loading although limited studies have analysed in detail how, and to what extent blast-structure interaction influences PBI risk. Furthermore, the suitability of criteria based on ideal assumptions has not yet been analysed. These knowledge gaps are increasingly important as researchers modelling urban blast scenarios with high levels of sophistication seldom question the validity and applicability of injury criteria for predicting the spatial extent of blast injuries. Further work is needed to determine how, and to what extent, modified blast loading conditions affects the risk of PBI. The challenges and limitations of using injury criteria based on idealised blasts should also be explored, with a view to distinguish the problematic features of blast waveforms for predicting injury risk.

This paper presents a numerical study to investigate the effects of blast interaction with a rigid corner structure, based on and verified through comparison to the experimental work of Gajewski & Sielicki [10]. CFD analysis was used to model blast interaction with and without (free-field) the corner structure, plus the additional case of a corner with a rigid wall along the entire length of the domain. The aim of this work is to quantify and analyse the effect on loading parameters at certain locations, the effect this has on expected PBIs, and the suitability and limitations of using available injury criteria.

2. Methodology

2.1 Overview

The experimental work by Gajewski & Sielicki [10] was used as a case study to numerically investigate structural-blast interaction effects resulting from an explosion detonating near a rigid building corner (Fig. 1). Gajewski & Sielicki investigated blast interaction and shielding effects provided by a rigid building corner, examining blast waves from the detonation of 200g and 400g TNT charges. Overpressure histories were measured at 4 locations around the corner structure.

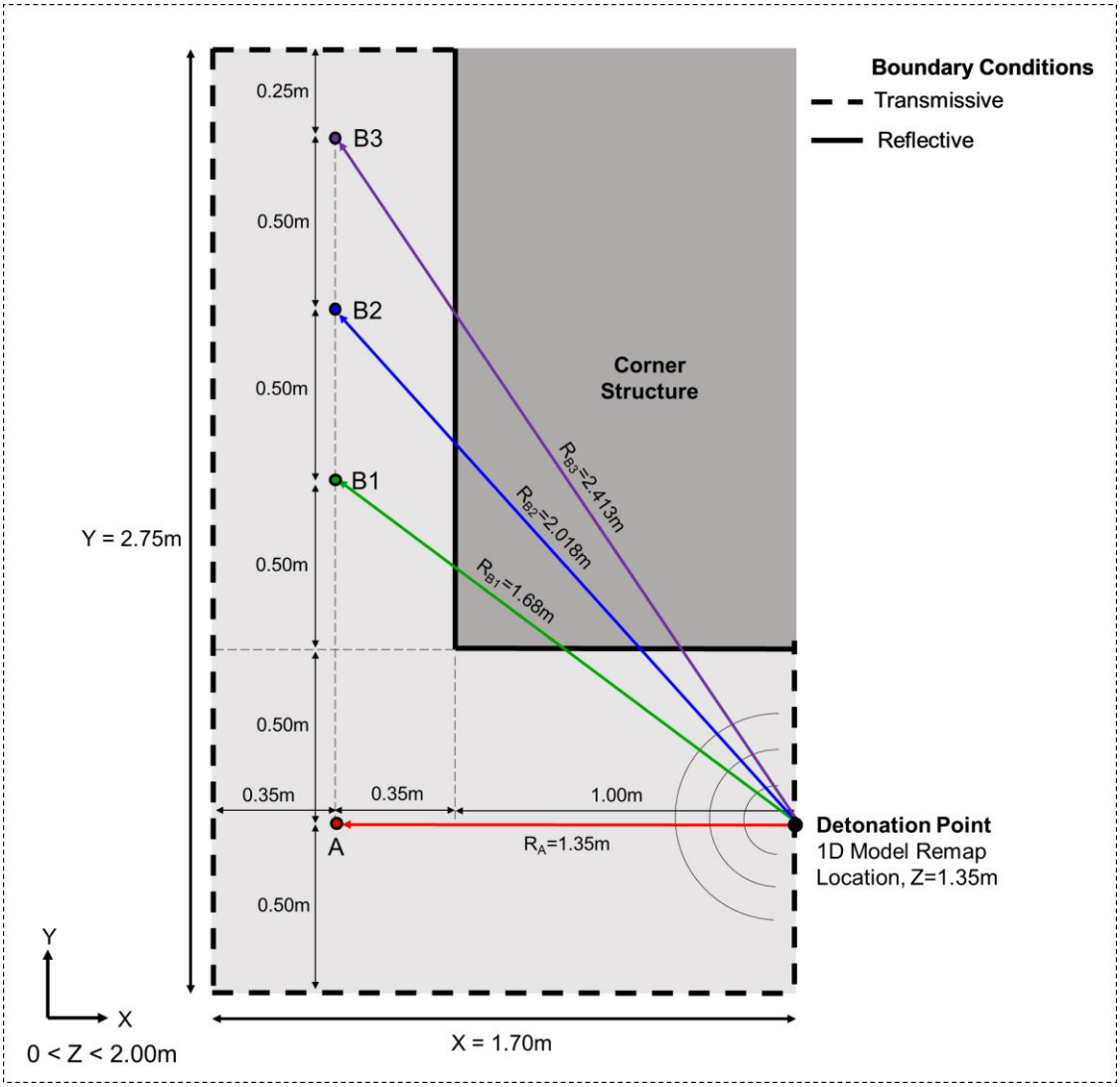

Fig. 1: Plan view schematic of the corner modelling scenario, detonation point and pressure monitoring locations at a height z=1.35m above the ground surface.

CFD analyses were undertaken to model blast wave interaction with a corner geometry resulting from the detonation of a 400g TNT charge, analogous to the experiments (Fig. 1). Two additional series of CFD analyses modelled the same explosive detonation, though examined two different scenarios: (i) without the corner structure to examine the free-field blast propagation scenario, and (ii) with the corner structure and an additional wall (running along the entire length of the bottom of the domain, i.e. y=0, as in Fig. 2) to examine channelling effects. The free-field scenario was modelled as opposed to using semi-empirical relations [11], [12] in order to resolve ground reflection effects and to permit direct comparison between simulations. Comparison between the three modelling scenarios

examined the extent that overpressure histories were modified by interaction with the corner (and additional wall) and the corresponding effect on primary blast injury (PBI) risk and limitations of using injury prediction criteria.

Overpressure histories were measured at four locations (A, B1-B3) surrounding the rigid corner structure (Fig. 1) consistent with the experimental setup. Gauge A was positioned in direct line-of-sight of the detonation, whereas gauges B1, B2 and B3 were located at successive distances around the corner, thus examining blast shielding effects (Fig. 1). The detonation point and pressure gauges were positioned at height z=1.35m above the ground surface; this was designed to represent the height of the chest centre for a standing position or the eardrums for an aiming-kneeling position, for a medium-sized person [10].

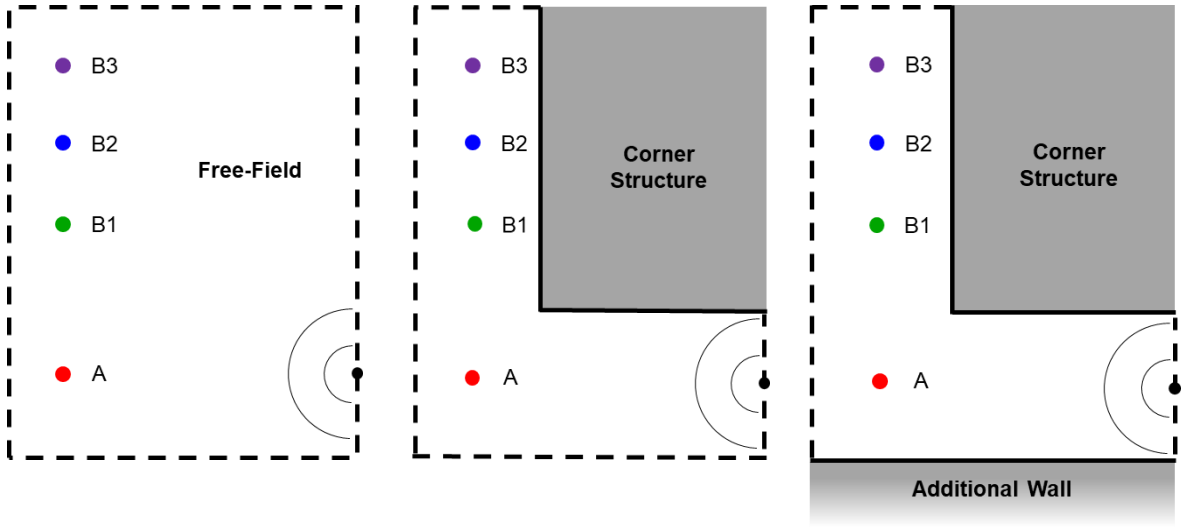

(a) Free-field Model (b) Corner Model (c) Corner & Wall Model

Fig. 2: Plan view schematics of each blast scenario modelled.

For each gauge location, PBI risk was interpreted through inspection of blast wave parameters and with reference to pre-defined injury criteria. Selected injury criteria were compiled and reviewed in [13], [14] and grouped into: (1) the auditory system; (2) pulmonary injury & lethality; and (3) brain-related PBI (Table 1).

Table 1: Summary of primary blast injury (PBI) criteria used to assess PBI risk.

Blast Injury Area	**Criteria Description**
Auditory System	**Peak Overpressure Thresholds** • 35 kPa [15] - Threshold for eardrum rupture • 103 kPa [15] - 50% probability of eardrum rupture • 202 kPa [16] - 100% probability of eardrum rupture
Pulmonary Injury & Lethality	**Peak Overpressure-Positive Phase Duration Functions** Bowen curves [17] for pulmonary (lung) blast injuries assuming a 70kg man stood near a wall, including: • Threshold for pulmonary blast injury • 1%, 50% and 99% probability of fatality
Brain-related PBI	**Peak Overpressure Thresholds** • 144 kPa [18] - 50% risk of mild brain haemorrhage

2.2 Numerical Modelling Methodology

ANSYS Autodyn [19] (Version 2020 R1) was used to perform CFD analyses in a two-stage approach. Firstly, the detonation of a 400g spherical TNT charge was modelled as a one-dimensional (1D) CFD analysis comprising a spherical free-air explosion to model the early-stage (R<0.5m) blast wave propagation. Secondly, three-dimensional (3D) inviscid Eulerian

CFD analyses 'remapped' the 1D incident blast wave to propagate within the domain to interact with the corner geometry (and wall), including blast reflections at the corner walls and ground surface.

Detonation & Near-Field (R<0.5m) Blast Propagation (1D Model)

A radially symmetric 1D wedge domain was used to model detonation and subsequent blast wave propagation in air, to a distance of 0.5m corresponding to the blast wave propagation to the nearest reflective surface, the wall (Fig. 1). A wedge domain of length, L=2.0m was necessary to provide sufficient space to capture the entire blast wave history to evaluate impulse. A sphere of TNT material was assigned at the apex of the wedge domain containing atmospheric air elements, such that the explosion and resulting shockwave propagated towards the open end (Fig. 3). An 'outflow' boundary condition was assigned to the distal end to allow air to exit after being accelerated by the shock wave, although the simulation was terminated before end expansion waves had reached the gauge location.

Default values for the TNT and air equations of state (EOS) were used in the computations and retrieved from the standard Autodyn library (Table 2). The TNT material was modelled using the Jones-Wilkins-Lee (JWL) equation of state (EOS) [20]. Air was modelled as an ideal gas with an ambient pressure of 101.33 kPa by specifying an internal energy of 2.068×10^5 mJ/mm^3 (Table 2). The multi-material Euler-Godunov solver was used to model both the detonation of explosive material and subsequent shock wave propagation through air. A pressure gauge was defined within the wedge domain at a standoff distance of 0.5m to monitor mesh sensitivity effects and to compare with empirical blast wave calculations [11], [12].

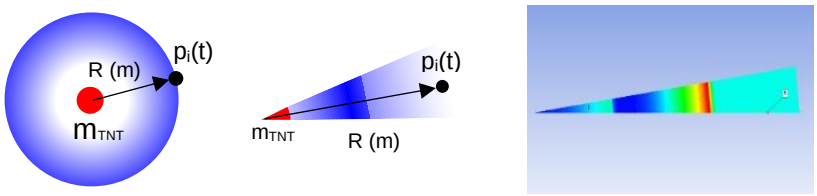

(a) Assumed free-air spherical detonation. (b) 1D wedge domain schematic. (c) 1D radial blast propagation within wedge domain.

Fig. 3: 1D model of the detonation and early-stage blast propagation assuming a spherical free-air detonation.

Table 2: Material Equations of State for air and TNT.

	Air	**TNT**
Equation of State	Ideal Gas γ=1.4 ρ=1.225x10^{-3} mg/mm^3 Remainder as per material library	JWL As per material library
Initial Conditions	Internal energy = 2.068x10^5 mJ/mm^3 Initial Temperature = 288°K (15°C)	Default

Sensitivity studies were undertaken to assess the effect of mesh resolution on the blast wave parameters calculated at the 0.5m standoff distance (see Appendix-1D Mesh Sensitivity Study). Following verification, the CFD analysis was performed until the shock front propagated to a standoff distance of 0.5m, then saved as a remap file (.FIL) to be utilised as initial conditions for subsequent 3D analyses.

Blast Wave Propagation (R>500mm) & Structural Interaction (3D Models)

The 3D modelling domain was defined and filled with air modelled as an ideal gas. The 1D model datafile was 'remapped' into the 3D domain using coordinates for the detonation point corresponding to the experimental setup (Fig. 1). Again, a multi-material, 3D Euler-Godunov solver was adopted so both air and detonation products were modelled from the remapped 1D analysis data.

The rigid corner was modelled using void cells, forming a cuboid obstacle with dimensions consistent with the experiments (Fig 1). By default, void cells have reflective boundary conditions, thus modelling a perfectly rigid structure with reflective surfaces. Pressure monitoring points were assigned at four locations (A, B1, B2 and B3) in the domain using 3D cartesian coordinates corresponding to the reference experimental setup (Fig 1). A reflective boundary condition was assigned to the lower z-plane of the domain to model the ground surface, and transmissive "flow out" boundary conditions were assigned to all other exterior domain boundaries to model free-field (unobstructed) blast wave propagation.

The free-field scenario without the corner structure was modelled by removing the block of void cells. The corner & wall scenario was modelled by specifying a reflective boundary condition to the y=0 plane, thus representing a rigid wall along the bottom edge of the modelling domain (Fig. 2).

As found in other CFD studies [22], [23], transmissive boundary conditions were not fully effective, with some localised reflection occurring at the domain sides. Outer dimensions of the 3D domain therefore had to be defined sufficiently large to reduce any potential boundary perturbations from interfering with regions of interest, particularly in the vicinity of pressure gauge locations. An iterative approach was taken during the development of the 3D model to optimise the domain size to provide sufficient space to reduce unwanted boundary interference effects while reducing the computational expense of the modelling problem.

Preliminary models indicated that pressure histories were sensitive to boundary perturbations at the 'ceiling' of the model (upper z plane). The total vertical height of the modelling domain was therefore defined as 2.0m to allow sufficient space above the detonation plane (z=1.35m) to reduce the influence of boundary interference on blast propagation and pressure calculations. Similarly, spacing was required adjacent to gauge locations (0.35m). Following these observations, the 3D modelling domains comprised exterior dimensions of 1.7m x 2.75m x 2.0m (Fig 1).

Sensitivity studies were undertaken to optimise the mesh size and verify the accuracy and reliability of the 3D model of the corner blast scenario (see Appendix-3D Mesh Sensitivity Study). Mesh convergence was observed for element dimensions of 5x5x10mm, giving rise to a total of 37.7 million elements within the modelling domain.

Following verification and sensitivity studies, all models were specified with consistent setup conditions (i.e. mesh configuration, remap location, material properties and pressure gauge locations) to allow direct comparison between the model results. The 3D CFD models were simulated for a duration of t=7.0ms, which allowed sufficient time for the primary blast wavefront to propagate around the corner and pass the furthest measurement location, B3 (Fig. 1). Pressure data was recorded at time increments of 0.02ms, consistent with the experimental data; this provided adequate resolution of pressure histories while maintaining manageable data storage. Simulation run times for the final model with 37.7 million elements required ≈660 CPU hours and ≈64GB RAM.

3. Results

3.1 Verification of the Corner Model

Calculated peak overpressure and peak specific impulse for each gauge location are plotted in Fig. 4 and overlaid with experimental data from [10]. Peak overpressure and peak specific impulse were observed to decrease with radial stand-off distance and increasing distance around the corner in agreement with experimental data (Fig. 4). Decreasing peak pressures and impulses are expected with increasing stand-off distance although an enhanced reduction was observed due to shielding from the corner structure.

Peak overpressures calculated by the CFD model show fair agreement with the experimental data although values were slightly below the experimental mean values, although with relatively small absolute differences (Fig 4a; Table 3). Calculated peak specific impulses demonstrated relatively better agreement with the experimental data (within 5 kPa.ms of mean), although typically exhibited reduced values in comparison to experiments (Fig 4b; Table 3). Overall, noting the variability in the experimental data, the CFD model calculated peak overpressures and peak specific impulses with fair agreement and exhibited similar relationships with respect to different radial stand-off distance and locations surrounding the corner (Fig 4).

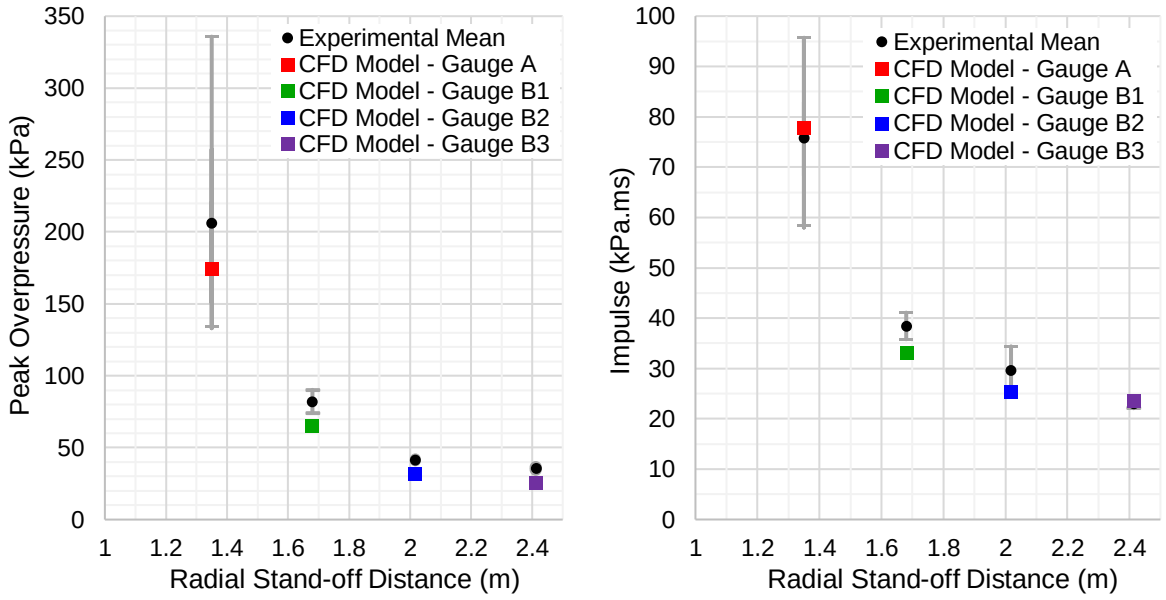

(a) Peak overpressure (b) Peak specific impulse

Fig. 4: Verifying corner model with experimental data from [10]: calculated peak overpressure and peak specific impulse at each gauge location.

Table 3: Verifying corner model with experimental data from [10]: calculated peak overpressure and peak specific impulse at each gauge location.

	Peak Overpressure, P_i (kPa)		**Peak Specific Impulse, I_i (kPa.ms)**	
Gauge	Experimental Mean [10]	Model	Experimental Mean [10]	Model
A	206.6 (134.0-335.8)	175.0	75.9 (58.3-95.7)	77.9
B1	82.2 (74.1-90.2)	65.6	38.5 (35.8-41.1)	33.2
B2	41.8 (41.1-42.7)	32.5	29.7 (25.8-34.4)	25.5
B3	35.8 (34.8-36.7)	26.2	23.2 (22.1-24.2)	24.3

3.2 Analysing blast-structure interaction effects on loading

Pressure contours show the primary shock front propagating from the detonation point towards gauge A, which is followed by reflections from the corner structure (Fig. 5a,b) and

also from the lower wall in the corner and wall scenario (Fig. 5c,d). Reflections were observed to catch-up and gradually merge with the primary shock front (Fig 5b,d) before diffracting around the corner structure upon reaching the corner vertex. Inspection of pressure contours shows that the diffracted wavefront had decreased pressure with proximity to the shielded corner surface.

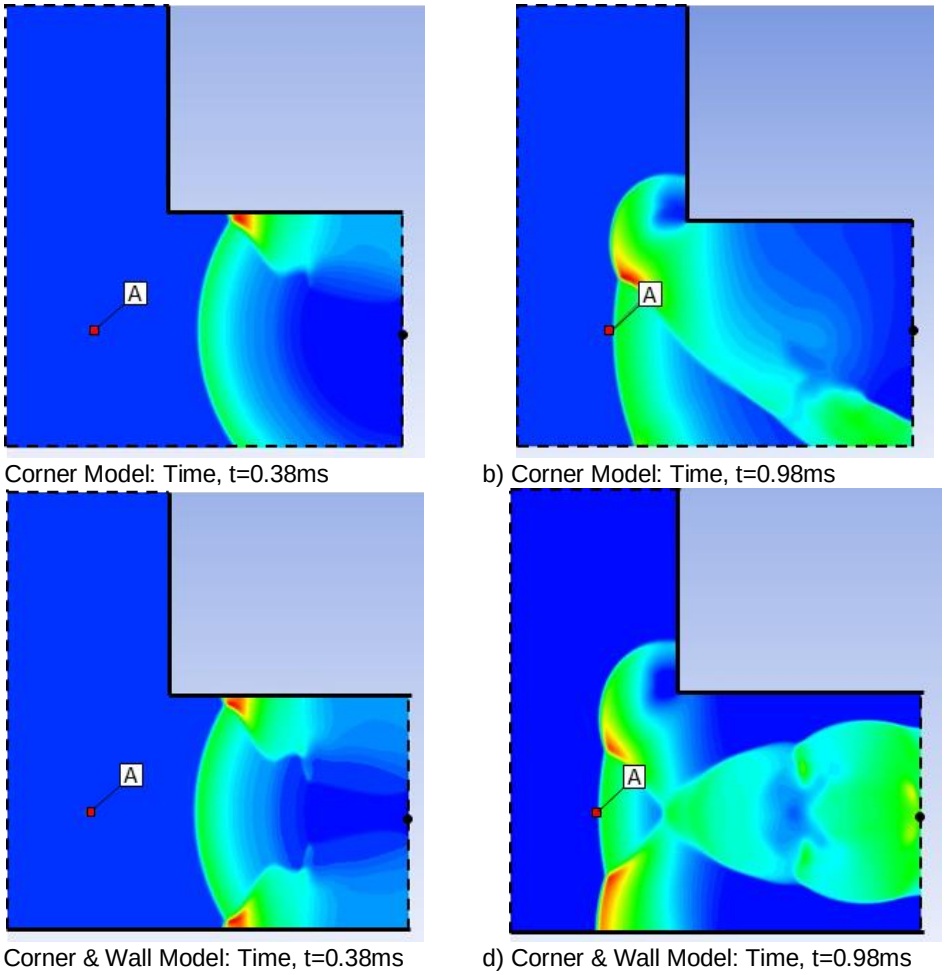

a) Corner Model: Time, t=0.38ms b) Corner Model: Time, t=0.98ms

c) Corner & Wall Model: Time, t=0.38ms d) Corner & Wall Model: Time, t=0.98ms

Fig. 5: Plan view (z=1.35m) of pressure contours at subsequent time intervals showing primary and reflected blast waves approaching gauge A.

Pressure histories calculated by CFD analyses were analysed to determine how the corner structure and the additional lower wall modified blast loading at each gauge location in comparison to the free-field scenario.

Gauge A

At gauge location A, initial peak overpressures were effectively the same (P_i≈175 kPa) for all modelling scenarios (Table 4a). This is due to gauge A being directly exposed to the unimpeded primary shock front, which is initially unaffected by the presence of the corner or the additional wall. For the corner scenario and the corner & wall scenario, a second pressure peak occurred ≈0.5ms after the primary shock front, as visible in Fig.6 b-c. Importantly, for the corner and wall scenario, this second pressure peak was 53.7% (270.4 kPa) higher than the primary wavefront (Table 4a). Peak specific impulse at gauge A was 38% higher for the corner scenario than the free-field, and 110.3% higher for the corner and wall scenario than the free-field (Table 4b). Significantly increased impulse and peak overpressure for the corner and wall scenario is attributed to channelling from the lower wall and corner, which effectively focusses blast reflections at gauge A, as visible in Fig. 5.

Table 4: Comparing loading parameters between the free-field scenario, the corner and the corner & wall scenarios at each gauge location.
a) Computed peak overpressures.

Radial Stand-off distance (m)	Gauge	**Peak Overpressure, P_i (kPa)**						
		Free-Field Model	**Corner Model**	% Difference*	**Corner & Wall Model****		% Difference*	
1.35	A	175.9	175.0	-0.5%	176.0	270.4	0.1%	53.7%
1.68	B1	114.9	65.6	-42.9%	65.2	81.6	-43.3%	-29.0%
2.02	B2	80.5	32.5	-59.6%	32.3	70.8	-59.9	-12.0%
2.41	B3	61.8	26.2	-57.6%	25.8	61.5	-58.2%	-0.5%

b) Computed peak specific impulse.

Radial Stand-off distance (m)	Gauge	**Peak Specific Impulse, I_i (kPa.ms)**				
		Free-Field Model	**Corner Model**	% Difference*	**Corner & Wall Model**	% Difference*
1.35	A	56.3	77.9	38.3%	118.4	110.3%
1.68	B1	53.2	33.2	-37.6%	143.1	169.0%
2.02	B2	49.9	25.5	-48.8%	-	-
2.41	B3	47.1	24.3	-48.4%	-	-

* % Differences are with respect to free-field scenario.
** Pressure histories from the Corner & Wall model exhibited primary and secondary pressure peaks

Gauges B1-B3

Inspection of the overpressure histories at gauges B1-B3 shows that blast interaction with the corner resulted in a delayed shock front arrival in comparison to the free-field model (Fig. 6c-k). This delay represents the additional time required for the blast wave to diffract around the corner and propagate over a longer distance in comparison to the direct radial distance in the free-field scenario.

For the corner scenario, blast wave interaction with the corner caused a shielding effect at gauges B1-B3 with significantly reduced peak overpressure and lower peak specific impulse in comparison to the free-field scenario (Table 4). Peak overpressures were reduced by 43%-60% at locations B1-B3 behind the corner in comparison to the free-field scenario (Table 4a). Peak specific impulses at gauges B1-B3 were 38%-48% less than the equivalent free-field scenario (Table 4b). Overpressure histories at B1-B3 in the corner scenario resulted in reduced cumulative and peak specific impulses in comparison to the free-field, although positive phase duration remained effectively the same (Fig 6).

For the corner and wall scenario, interaction of the primary shock front with the corner caused a similar shielding effect at gauges B1-B3, leading to effectively the same overpressures as the corner model (Table 4a). Like the corner model, primary peak overpressures were significantly reduced (43%-59%) in comparison to the free-field scenario (Table 4a). However, channelling from the additional wall caused a second series of pressure peaks (see Fig 6e,h,k) that all exceeded the primary wavefront overpressure in comparison to the corner alone (Table 4a). Taking into consideration the maxima of these successive pressure peaks, channelling from the corner and wall reduced the shielding effect of the corner with overpressures at B1-B3 reduced to a lesser extent (0.5-29%) relative to the free-field scenario (Table 4a).

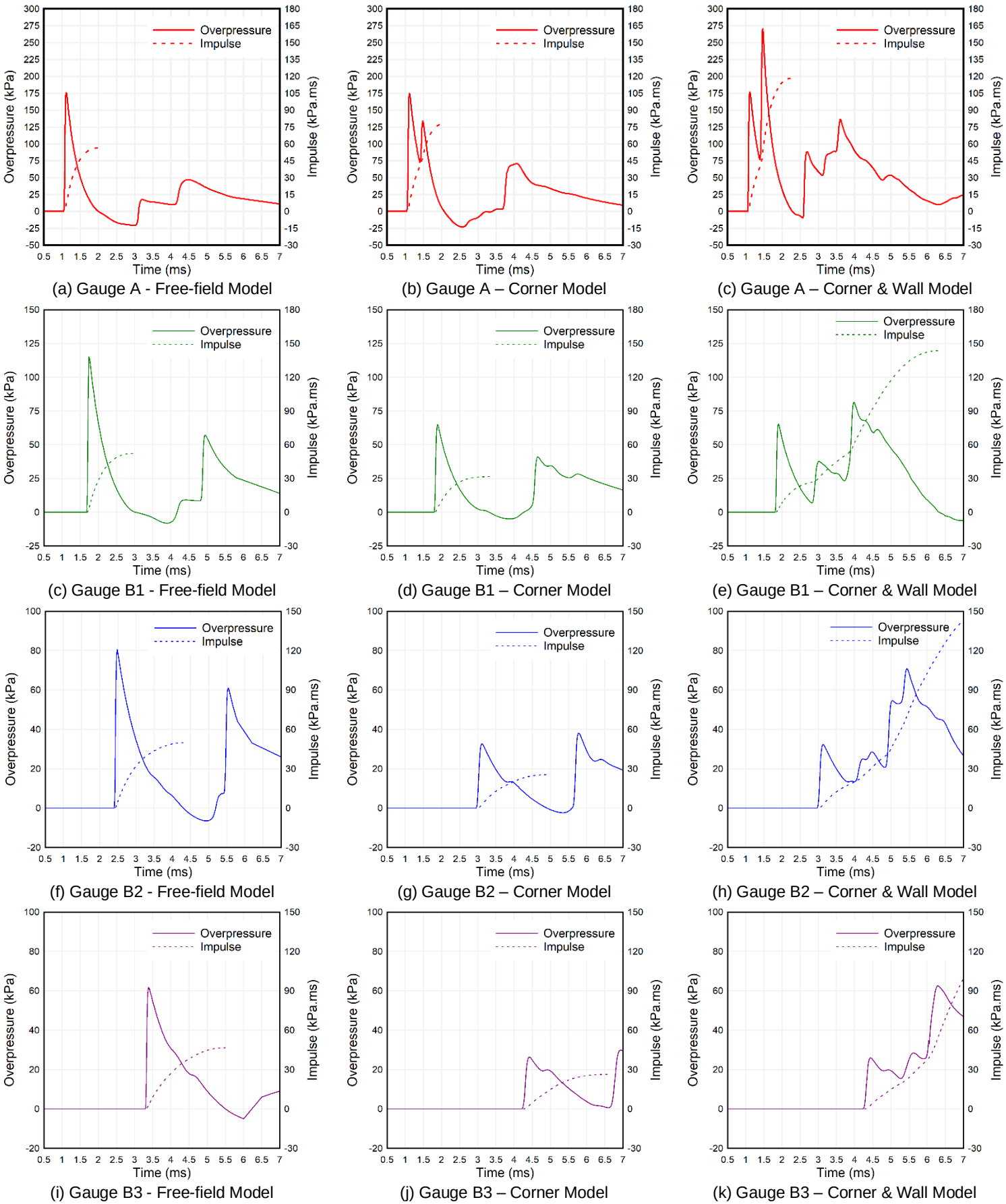

(a) Gauge A - Free-field Model
(b) Gauge A – Corner Model
(c) Gauge A – Corner & Wall Model
(c) Gauge B1 - Free-field Model
(d) Gauge B1 – Corner Model
(e) Gauge B1 – Corner & Wall Model
(f) Gauge B2 - Free-field Model
(g) Gauge B2 – Corner Model
(h) Gauge B2 – Corner & Wall Model
(i) Gauge B3 - Free-field Model
(j) Gauge B3 – Corner Model
(k) Gauge B3 – Corner & Wall Model

Fig. 6: CFD model overpressure and cumulative impulse histories at each gauge and each blast scenario.

Overpressure histories at B1-B3 for the corner and wall scenario demonstrated increasingly complex waveforms featuring multiple pressure peaks with extended positive phase durations, or durations (and impulses) that could not be resolved due to unreasonable computational demand (Fig 6). Importantly, peak specific impulses at gauges A and B1 were 110.3% and 169% higher than the free-field scenario (Table 4b). Inspection of pressure histories (Fig 6e,h,k), confirms that the significantly higher peak specific impulses in the corner & wall scenario are due to the arrival of later-stage overpressures (i.e. ≈2ms after shock arrival at B1-B3).

4. Discussion

Blast-structure interaction effect on primary injury risk

For each gauge location, primary blast injury (PBI) risk was determined by plotting blast wave parameters calculated in each CFD model with pre-defined PBI criteria (Fig. 7), adopting the graphical method for PBI prediction as developed in [13]. Expected PBIs at each gauge location for each blast scenario are summarised in Table 5.

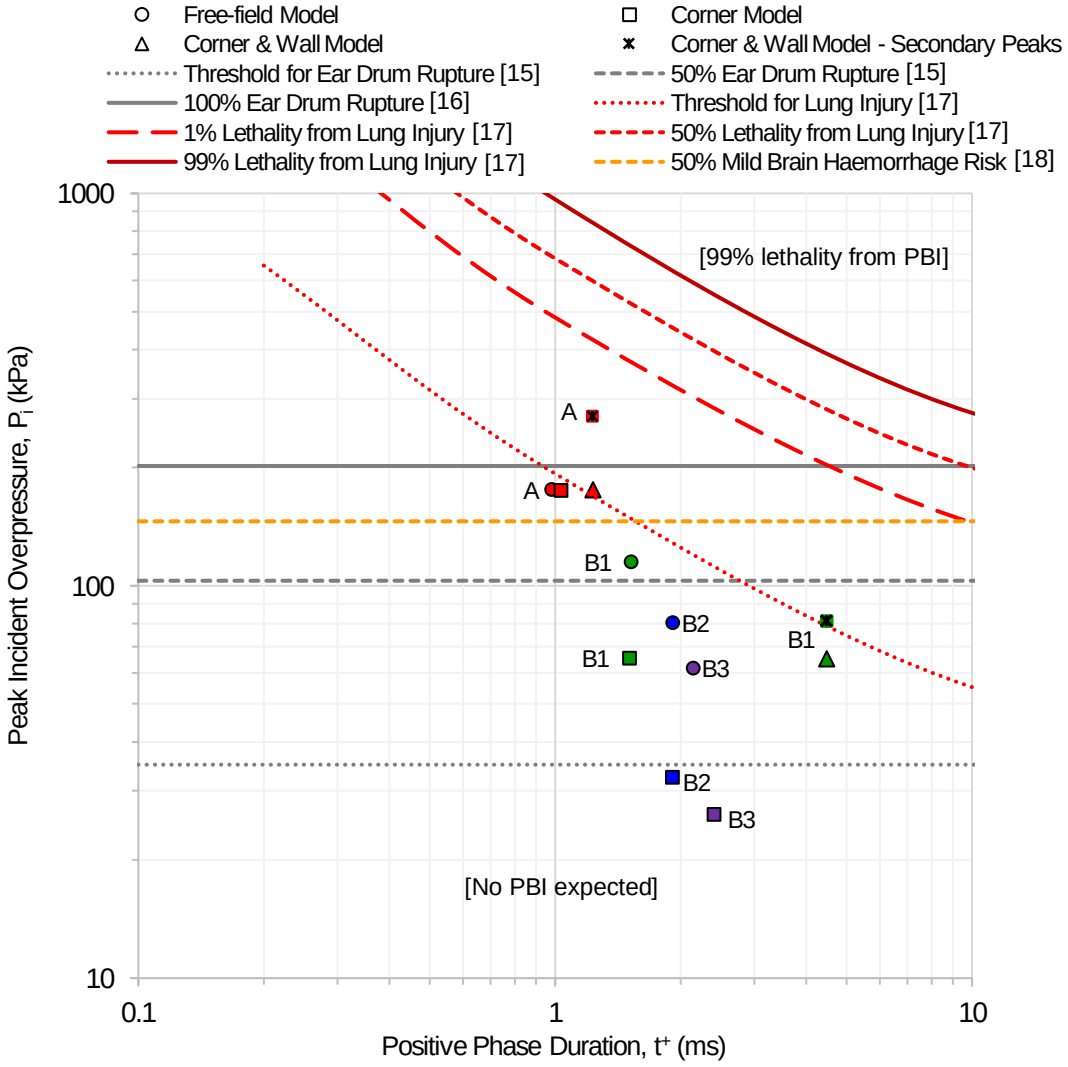

Fig. 7: Expected primary blast injury (PBI) risk at each gauge location for each blast scenario using blast parameters calculated by CFD models.

For the free-field and corner scenarios, the risk of PBI at gauge A was the same since the peak overpressure and positive phase duration remained effectively unchanged. From inspection of Fig. 7, blast parameters at gauge A correspond to the threshold conditions for pulmonary (lung) injury and there is over a 50% probability of mild brain haemorrhage and ear drum rupture. For the corner and wall scenario, when the secondary pressure peak (maximum) is considered, risk of pulmonary blast injury is significantly increased towards a 1% risk of fatality (Fig. 7).

For the corner blast scenario, reduced peak overpressures at gauges B1-3 due to shielding results in lower risk and severity of expected PBIs at all three gauges in comparison to the free-field scenario (Fig. 7). At gauge B2 for example, a lower peak overpressure in the corner scenario reduced the risk of ear drum rupture from almost 50% (free-field scenario) to below the threshold level, thus ear drum injury would no longer be expected (Fig. 7). Such shielding effects are believed to have occurred in the 2020 Beirut blast where shielding from the grain silos and other high-rise structures are thought to have mitigated harm [24].

Table 5: Summary of expected PBIs at each gauge location for each blast scenario.

Blast Scenario	Expected Risk of Primary Blast Injury (PBI) at Each Gauge			
	A	**B1**	**B2**	**B3**
Free-Field	Near 100% risk of eardrum rupture >50% risk of mild brain haemorrhage Near threshold for lung injury	>50% risk of eardrum rupture	<50% risk of eardrum rupture, but over threshold	<50% risk of eardrum rupture, but over threshold
Corner	As above (same as free-field)	<50% risk of eardrum rupture, but exceeds threshold	No PBIs expected	No PBIs expected
Corner & Wall	As above with: *100% risk of eardrum rupture *Near 1% fatality risk from lung injury	As above with: *threshold for lung injury	N/A	N/A

*Taking secondary pressure peaks (maximum overpressure) into account.

For the corner and wall scenario, peak overpressure at B1 is effectively the same as the corner model, although an increased positive phase duration is associated with an increased PBI risk. When the secondary (maximum) pressure peak at B1 in the corner and wall scenario is considered, injury risk increases further to the threshold for lung injury (Fig. 7, Table 5). Injury risk at gauge location B2 and B3 of the corner & wall scenario could not be calculated as the blast waveforms were complex such that positive phase durations could not be determined.

Overall, analysis has shown that in comparison to the free-field scenario, the corner significantly reduces injury risk at B1-B3 (behind the corner) due to shielding. However, in the corner and wall scenario, channelling caused secondary and successive pressure peaks with increased magnitude. This had the effect of significantly increasing injury risk at gauge A and reduced the protective shielding effect at gauge locations behind the corner, in comparison to the corner alone. While beyond the scope of this study, it is likely that shielding from the corner would also provide protection from fragmentation.

5. Limitations & Further Work

It should be recognised that other configurations and layouts of obstacles and structures will give rise to a wide range of interaction and loading effects. Importantly, alternative layouts can magnify loading conditions including increased peak overpressure, stagnation pressures and longer positive phase durations, which are associated with increased injury risk. This study was also limited to the investigation of blast interaction phenomena assuming perfectly rigid structures, neglecting the effects of structural deformation or frangibility, which would also influence loading modification.

The extent of loading modification following blast interaction with structures therefore depends on the individual scenario, layout and configuration of structures amongst many other factors. With so many variables and potential scenarios, it is challenging to predict the consequences in terms of injury risk and severity without knowledge or fast-running tools to estimate blast loading conditions. Further research is therefore needed to develop understanding of different urban blast scenarios to determine the sensitivity of different factors and variables (i.e. upper and lower bounds) and the subsequent consequences this has on injury from a probabilistic basis. Further understanding of complex blast loading effects and the impact on blast injury would support the development of more advanced predictive models, inform requirements for protection and hazard preparedness.

5.2 Suitability and limitations of existing PBI criteria

At present, PBI criteria are limited to estimating the likelihood of injury or fatality for a person subjected to a single, idealised blast pressure profile arising from detonations occurring in a free-field environment. Application of these PBI criteria rely on peak pressure and duration input parameters, which may not be appropriate or valid for complex waveforms. Through analysis of individual pressure histories in this study, a range of specific challenges and limitations were identified relating to the suitability of existing injury criteria when applied to complex blast scenarios.

At gauge location A, peak overpressures and positive phase durations remained effectively consistent, however, waveforms measured in the corner scenario and the corner and wall scenario exhibited non-trivial secondary pressure peaks and a 38% and 110% higher peak specific impulse respectively (Table 4b). While some injury criteria include blast impulse [15], the majority do not, and typically require inputs of peak overpressure and duration parameters. Importantly, higher impulse represents increased energy and momentum transfer [25], which may influence injury mechanisms and health outcomes. There is also a danger that these complex features of a modified blast waveform (i.e. multiple peaks and increased peak specific impulse) will not be accounted for when using existing injury criteria as they typically only require peak overpressure and duration as input parameters, resulting in unreliable injury predictions.

At gauge A, interaction with the corner caused secondary peak overpressures representing a non-trivial injury risk, or in the case of the corner and wall scenario, a significantly increased injury risk. Even for simple free-field scenarios, analysis of pressure histories in this study demonstrated that ground reflections generated secondary blast waves with peak overpressures associated with injury risk. This raises important questions about how to interpret existing PBI criteria that assume exposure to a single blast wave when secondary and successive peaks in overpressure occur. At present, there is no understanding of the effects of exposure to multiple blast waves on injury, and whether successive exposures are associated with cumulative injury.

As a result, blast waveforms that contain multiple pressure peaks or a positive phase duration that is extended or less clearly defined, such as those found in the corner and wall scenario, present a significant challenge and reduced confidence in predicting injury outcomes. Blast waves at gauges B1-B3 maintained a more ideal waveform following

interaction with the corner alone, suggesting that application of injury criteria may be valid and sufficiently reliable in simple scenarios where interaction effects are less.

5.3 Future Work

As demonstrated in this study, several challenges and uncertainties exist when applying traditional PBI criteria to 'complex' blast loading cases that arise in urban blast scenarios. To address these shortcomings, future work could investigate the potential for scaling methods to 'translate' criteria for increased reliability when applied to 'complex' conditions arising in urban scenarios. Sensitivity studies could provide additional understanding of confidence levels and reliability of PBI criteria when applied to different blast scenarios. It may be necessary for entirely new PBI criteria to be defined for complex blast waveforms, for example, to examine the cumulative physiological effects of multiple sequential blast exposures. In all cases, the large range of potential variables will make any developments challenging and care should be taken to prevent informing terrorist activity.

6. Conclusion

This study has examined the effects of blast interaction with a rigid corner and a wall in comparison to a free-field scenario and quantified loading modification at different locations. Existing PBI criteria were used to estimate the effects of modified loading on injury risk and severity, with further analysis to evaluate the suitability of injury criteria when applied to complex loading conditions.

Numerical models confirmed that blast interaction with the corner structure and an additional wall significantly modified loading parameters at all locations. Shielded gauges, located behind the corner, measured reduced peak pressures and impulses, which corresponded to a significantly reduced risk and severity of PBI. Gauges behind the corner maintained ideal-type waveforms following blast interaction with the corner, suggesting application of PBI criteria remained valid. Blast interaction with the corner and wall caused channelling leading to overall higher pressures and impulse in comparison to the corner alone. Complex waveforms featuring multiple peaks and increased peak specific impulse occurred at the exposed location (gauge A) and gauges B1-B3 (for the corner and wall scenario) which identified specific challenges and reduced reliability for injury prediction, defining recommendations for future work.

As CFD blast modelling capabilities continue to advance, this study provides important awareness and understanding of the limitations of using existing injury criteria to predict PBIs. Findings from this study raise awareness for researchers modelling injury risk in urban environments and highlights further areas of research required to improve understanding of complex blast loading conditions on injury risk and outcomes.

References

[1] S. E. Rigby *et al.*, “Preliminary yield estimation of the 2020 Beirut explosion using video footage from social media,” *Shock Waves*, vol. 30, no. 6, pp. 671–675, 2020.

[2] Action on Armed Violence (AOAV), “Explosive violence in 2019,” *AOAV*, 2020. [Online]. Available: https://aoav.org.uk/2020/explosive-violence-in-2019/.

[3] H. R. Champion, J. B. Holcomb, and L. A. Young, “Injuries from explosions: Physics, biophysics, pathology, and required research focus,” *J. Trauma - Inj. Infect. Crit. Care*, vol. 66, no. 5, pp. 1468–1477, 2009.

[4] P. Peters, “Primary Blast Injury: An Intact Tympanic Membrane Does Not Indicate the Lack of a Pulmonary Blast Injury,” *Mil. Med.*, vol. 176, pp. 110–114, 2011.

[5] G. Valsamos, M. Larcher, and F. Casadei, “Beirut explosion 2020 : A case study for a large-scale urban blast simulation,” *Saf. Sci.*, vol. 137, no. November 2020, p. 105190, 2021.

[6] F. G. Friedlander, “The Diffraction of Sound Pulses. II. Diffraction by An Infinite Wedge,” *Proc. R. Soc. London A Math. Phys. Eng. Sci.*, vol. 186, no. 1006, pp. 344–351, Sep. 1946.

[7] H. Axelsson and J. T. Yelverton, “Chest Wall Velocity as a Predictor of Nonauditory Blast Injury in a Complex Wave Environment,” *J. Trauma*, vol. 40, no. 3S, pp. 31S-37S, 1996.

[8] E. Li, A. Yoshinaka, and T. Josey, “Weathervane: a single point model for blast injury approximations,” in *20th Symposium on Military Aspects of Blast and Shock*, 2008.

[9] J. A. Teland, “Review of blast injury prediction models,” Norwegian Defence Research Establishment (FFI), 2012.

[10] T. Gajewski and P. W. Sielicki, “Experimental study of blast loading behind a building corner,” *Shock Waves*, no. 0123456789, 2020.

[11] C. N. Kingery and G. Bulmash, “Airblast Parameters From TNT Speherical Air Burst and Hemispherical Surface Burst, Technical Report ARBRL-TR-02555,” 1984.

[12] D. W. Hyde, “Conventional Weapons Program (ConWep).” Vicksburg: US Waterways Experimental Station, 1991.

[13] J. W. Denny, A. S. Dickinson, and G. S. Langdon, “Guidelines to inform the generation of clinically relevant and realistic blast loading conditions for primary blast injury research,” *BMJ Mil. Heal.*, vol. 0, no. 0, p. 6, 2021.

[14] J. W. Denny, A. S. Dickinson, and G. S. Langdon, “Defining blast loading ‘zones of relevance’ for primary blast injury research: A consensus of injury criteria for idealised explosive scenarios.,” *Med. Eng. Phys.*, vol. 93, pp. 83–92, 2021.

[15] US Department of Defense (DoD), “UFC 3-340-02, ‘Structures To Resist The Effects Of Accidental Explosions,’” Washington, D.C., 2008.

[16] J. H. Jensen and P. Bonding, “Experimental pressure induced rupture of the tympanic membrane in man,” *Acta Otolaryngol.*, vol. 113, no. 1–2, pp. 62–67, 1993.

[17] I. G. Bowen, E. R. Fletcher, and D. R. Richmond, “Estimate of Man’s Tolerance to the Direct Effects of Air Blast.,” Washington, D.C., 1968.

[18] K. A. Rafaels *et al.*, “Brain injury risk from primary blast,” *J. Trauma Acute Care Surg.*, vol. 73, no. 4, pp. 895–901, 2012.

[19] Century Dynamics, “AUTODYN.” 2011.

[20] E. L. Lee, H. C. Hornig, and J. W. Kury, “Adiabatic Expansion of High Explosive Detonation Products (Report UCRL-50422),” 1968.

[21] P. C. Dobratz, B. M. and Crawford, “LLNL explosives handbook: properties of chemical explosives and explosives and explosive simulants,” 1985.

[22] J. W. Denny and S. K. Clubley, "Evaluating long-duration blast loads on steel columns using computational fluid dynamics," *Struct. Infrastruct. Eng.*, vol. 0, no. 0, pp. 1–17, 2019.

[23] S. E. Rigby *et al.*, "A Numerical Investigation of Blast Loading and Clearing on Small Targets," *Int. J. Prot. Struct.*, vol. 5, no. 3, 2014.

[24] G. Sawaya, "beirut's grain silos: the monolith that shielded the city during 2020's port blast," *designboom*, 2021. [Online]. Available: https://www.designboom.com/architecture/beiruts-grain-silos-the-monolith-that-shielded-the-city-02-04-2021/. [Accessed: 04-Jan-2022].

[25] S. E. Rigby *et al.*, "Predicting the response of plates subjected to near-field explosions using an energy equivalent impulse," *Int. J. Impact Eng.*, vol. 128, no. January, pp. 24–36, 2019.

[26] D. W. Hyde, "ConWep: Conventional Weapons Effects (Application of TM 5-855-1)." US Army Corps of Enigneers, Waterways Experiment Station, Vicksburg, MS, 1992.

Appendix

1D Mesh Sensitivity Study

Mesh configurations ranging from 500-40,000 elements (element sizes ranging 0.05-4mm) were tested. Since no measurements were obtained at a 500mm standoff in the experiments, accuracy of the numerical blast wave was assessed by comparison to empirically-calculated blast parameters (Fig. A). The Kingery & Bulmash equations [11], automated in ConWep software [26], were used to calculate blast wave parameters for a 400g TNT spherical air burst at a 500mm stand-off distance. It was found that a wedge domain comprising 20,000 0.1mm elements demonstrated convergence and satisfactory agreement with empirical calculations for incident blast wave parameters (Fig. A).

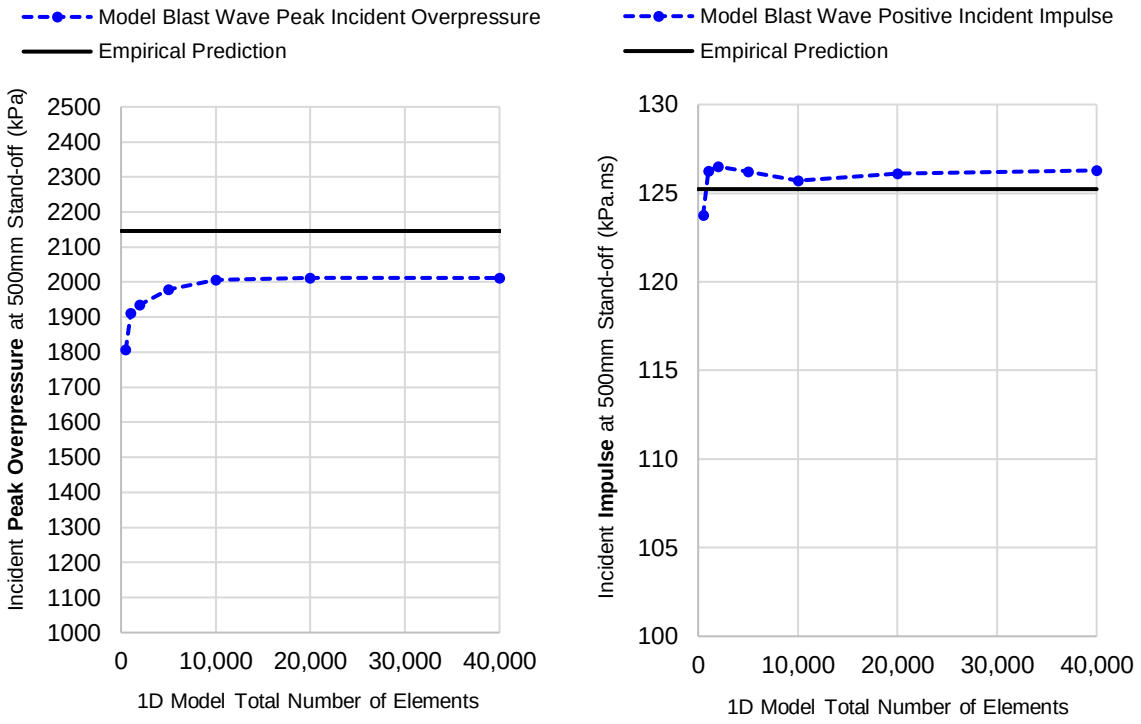

(a) Peak overpressure at 500mm Stand-off (b) Peak specific Impulse at 500mm Stand-off

Fig. A: 1D CFD Model Mesh Sensitivity Study: (a) peak overpressure and (b) peak specific impulse at 500mm stand-off vs. empirical predictions.

3D Mesh Sensitivity Study

Pressure histories at gauge location A were used to verify model performance for element dimensions from 20mm to 5mm, specifically, peak overpressure (Fig. B(i)) and total positive impulse (Fig. B(ii)) at gauge A (Table A).

Peak specific impulse values converged for element dimensions of 5x5x10mm, giving rise to a total of 37.7 million elements within the modelling domain. For this mesh configuration, peak specific impulse demonstrated good agreement with experiments by Gajewski & Sielicki [10], slightly exceeding the experimental mean by 2.5% (Table A). Fair agreement was also observed for the computed peak overpressure, which was 15.3% lower than the experimental mean and within the lower and upper bound experimental values (Table A, Fig. B).

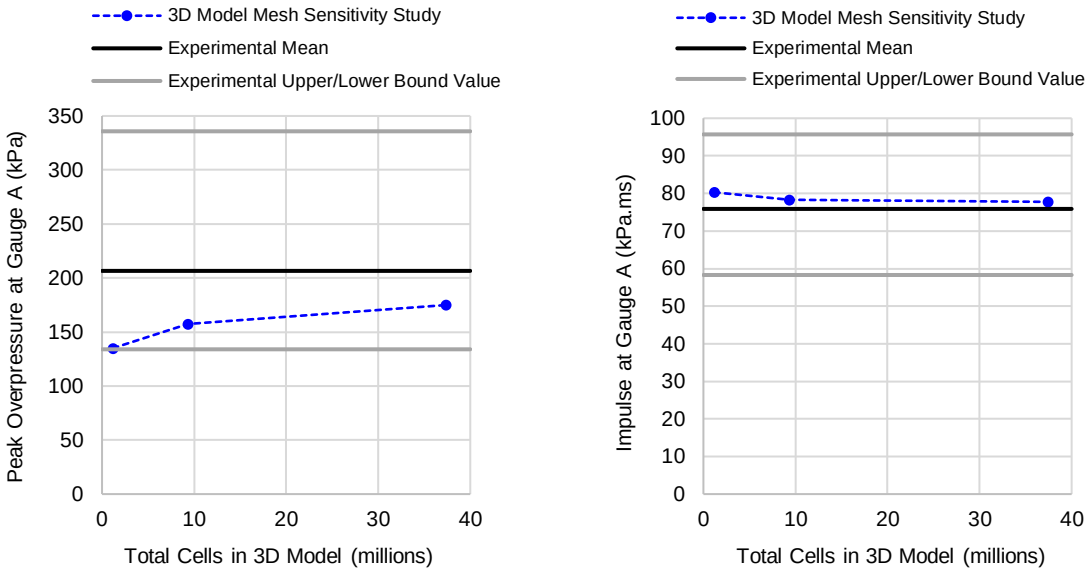

(i) Peak overpressure at Gauge A

(ii) Impulse at Gauge A

Fig. B: 3D CFD Model Mesh Sensitivity Study: (a) peak overpressure and (b) peak specific impulse at Gauge A vs. Experimental Data.

Table A Mesh Sensitivity Study: blast wave parameters at Gauge A vs Experimental Data [10].

Element Dimensions (mm)	**Total Number of Elements (million)**	**Peak Overpressure at Gauge A (kPa)**	**% Difference (To Experimental Mean)**	**Impulse at Gauge A (kPa.ms)**	**% Difference (To Experimental Mean)**
20x20x20	1.19	135.1	-34.6%	80.3	5.8%
10x10x10	9.35	157.3	-23.9%	78.3	3.2%
5x5x10	37.4	175.0	-15.3%	77.8	2.5%
Experimental Mean [10]		206.6 (134.0 - 335.8)		75.9 (58.3 - 95.7)	